UKAEA-CCFE-PR(22)12

Emmanuele Peluso, Andrea Murari, Teddy Craciunescu, Ernesto Lerche, Pasquale Gaudio, Michela Gelfusa, Dani Gallart, David Taylor, JET Contributors

Conditional recurrence plots for the Investigation of Sawteeth Pacing with RF Modulation

Conditional recurrence plots for the Investigation of Sawteeth Pacing with RF Modulation

Emmanuele Peluso, Andrea Murari, Teddy Craciunescu, Ernesto Lerche, Pasquale Gaudio, Michela Gelfusa, Dani Gallart, David Taylor, JET Contributors

This is a preprint of a paper submitted for publication in
Plasma Physics and Controlled Fusion

Conditional recurrence plots for the Investigation of Sawteeth Pacing with RF Modulaton

Emmanuele Peluso[1], Andrea Murari[2], Teddy Craciunescu[3], Ernesto Lerche[4,5], Pasquale Gaudio[1], Michela Gelfusa[1], Dani Gallart[6], David Taylor[7] and JET Contributors[§]

[1] Department of Industrial Engineering, University of Rome "Tor Vergata", via del Politecnico 1, 00133 Roma, Italy
[2] Consorzio RFX (CNR, ENEA, INFN, Universita' di Padova, Acciaierie Venete SpA), Corso Stati Uniti 4, Padova, Italy
[3] National Institute for Laser, Plasma and Radiation Physics, Magurele-Bucharest, Romania
[4] Euratom/CCFE Fusion Association, Culham Science Centre, Abingdon, United Kingdom,
[5] LPP-ERM/KMS, Association EUROFUSION-Belgian State, TEC Partner, Brussels, Belgium
[6] Barcelona Supercomputing Center (BSC), 08034 Barcelona, Spain
[7] Culham Centre for Fusion Energy, Oxford, United Kingdom

[§] See the author list of "Overview of JET results for optimising ITER operation" by J. Mailloux et al. to be published in Nuclear Fusion Special issue: Overview and Summary Papers from the 28th Fusion Energy Conference (Nice, France, 10-15 May 2021)

E-mail: emmanuele.peluso@uniroma2.it

Received xxxxxx
Accepted for publication xxxxxx
Published xxxxxx

Abstract

In many fields of the natural sciences, from biology to physics, advanced data analysis tools are acquiring more and more importance to investigate difficult problems. A typical application is synchronization experiments, which involve coupled quantities, a "target" and a "driver", with quasi-periodic behaviours. Unfortunately, in complex systems very rarely a couple of quantities can be really considered fully isolated and immune from other influences. It is therefore important to consider not only the legacy of their past, but also the possible effects of additional confounding factors. In order to tackle this problem, an advanced application of the recurrence plots, called Conditional Recurrence plots, has been developed. The potential of the innovative technique has been confirmed by comparison with the conditional transfer entropy, the traditional technique used to address these problems. Preliminary results from experimental data of sawteeth pacing with radio frequency modulation are very encouraging. Being quasi-periodic, sawteeth occurs naturally and, especially in H mode plasmas, the effectiveness of the pacing with radiofrequency heating can be difficult to establish. The proposed data analysis procedure is aimed at better discounting the confounding factors, like natural sawteeth, providing both a more accurate quantification of the pacing efficiency and a deeper insight into the physical processes involved, thanks to a better understanding of the relevant causal relations.

Keywords: Sawteeth Pacing, Conditional Transfer Entropy, Recurrence Plots, Non linear dynamics

1. Introduction

Nowadays magnetically controlled nuclear fusion reactors represent the most promising configuration to produce energy for general use in the not too far future. The next generation device, ITER, is expected to operate in an operation regime commonly called H-mode [1], where the confinement time, i.e. the average time during which the plasma loses its energy, is almost twice the one of the L-mode regime. However, the plasma core of these discharges is affected by reconnection events when the safety factor decreases below one. These instabilities leave a clear signature in the main plasma parameters and particularly in the temperature, as quite evident oscillations. It has been demonstrated that too long natural sawteeth periods can results in excessively large crashes, which can constitute the seed of neoclassic tearing modes (NTM) [2]. The growth and saturation of NTMs are then well known to have the potentiality to lead to catastrophic events known as disruptions [3]. The simple suppression of sawteeth on the other hand then, is probably not the best strategy in the perspective of the reactor, because they can contrast the accumulation of both ashes and impurities, which could lead to the consequent poisoning of the plasma core.

Recently, it has been observed at JET how notches in the ICRH heating scheme can effectively been used to pace sawteeth in L-mode discharges, by influencing the fast ions distribution of the minorities injected; the results have been quantified with both advanced and simple statistical techniques [4].

The H-mode phase is in general more complicated to analyse, because of a series of non-linear effects. However very good results have been described in [5] implementing advanced statistical tools such as the Transfer Entropy and the Convergent Cross Mapping [6]. In particular, the amount of Shannon information shared between the quantity denoted as the driver, the ICRH, and the response one, the electron temperature in the core (Te), was quantified. The main limitation of such estimators lies in the underlying hypothesis that only the considered driver, i.e. the ICRH, is influencing the observable response, i.e. the central electron temperature. In this article then, an original statistical tool has been applied to DD pulses during H-mode phases, to describe the ICRH pacing, by taking into consideration also the possible occurrence of natural sawteeth: the Conditional Joint Recurrence Plots [8]. This analysis is complemented by a more traditional technique, used already in the past to address this type of situations: the so-called Conditional Transfer Entropy [7].

This article is structured as follows. Section 2 provides a brief description of the pacing technique, then Section 3 describes Conditional Joint Recurrence Plots (CJRP) and the Conditional Transfer Entropy (CTE), while Section 4 shows the analysis performed as well as the estimates provided by the modelling code considered, i.e. the PION code[9], before drawing the conclusions.

2. Overview of sawteeth pacing experiments

Sawteeth are the visible effects on the main plasma parameters of the periodical relaxation of internal kink modes[10]. As it has been stated in the introduction, it has been observed experimentally [2] that too long sawteeth periods can lead to the large crashes with deleterious effects on the plasma confinement and even to its stability. Consequently, to keep the beneficial effects related to the expulsion of He ash and impurities, sawteeth pacing experiments have been performed and have demonstrated in the last years their effectiveness. Considering what stated about the sawteeth then, the objective of such experiments consists of triggering sawteeth crashes at specific rates in order to preserve their positive effects and reduce or avoid the unwanted consequences.

According to [11][12] the basic condition for a sawtooth to occur, can be summarized in terms of the shear $\left(s = \frac{r}{q}\frac{dq}{dr}\right)$ at the q=m=n=1 surface, where m and n are the poloidal and toroidal mode numbers, as follows:

$$s|_{q=1} > \max(s_{crit}, \delta\,\widehat{W}) \qquad (1)$$

Where s_{crit} is a critical shear value depending on physical quantities in a narrow layer close to the q=1 surface[11], namely the ion toroidal beta, the pressure and the density scale lengths considered, while $\delta\,\widehat{W}$ stands for the normalized potential energy:

$$\delta\widehat{W} \propto \frac{\delta W}{s_1 \xi^2 \hat{\rho}} \qquad (2)$$

where ξ represents the radial displacement inducing the perturbation, i.e. $\xi \simeq e^{im\left(\theta - \frac{n}{m}\phi\right)}$. Specifically then:

$$\delta W = \delta W_{core} + \delta W_{fast} \qquad (3)$$

Considering (2) and (3), to implement the pacing two typologies of experiments had been historically conducted aimed at either altering the shear close to the q=1 surface $\left(s_1 = s\,|_{q=1}\right)$ [13], or at modifying the fast ion population and consequently the δW_{fast} term[4][14]. The former type is based on modifying the local plasma parameter and the current profile close to the q=1 surface with the use of an external heating, such as the electron cyclotron (ECH)[13]. The latter instead, is based on the injection of a minority species in the plasma and on a ICRH heating scheme[4][14]. Results had been obtained by both varying the ICRH antenna phasings [14], or by directly notching the ICRH [4].

To consolidate the conclusions which can be derived from these experiments, a statistical evaluation of the correlation between the fast ion populations and the ICRH is therefore of great interest.

3. Conditional Transfer Entropy and Conditional Joint Recurrence Plots

In this section the two main statistical estimators, the Conditional Joint Recurrence Plots and the Conditional Transfer Entropy are described in subsection 3.1 and 3.2 respectively.

3.1 Recurrence Plots and Conditional Recurrence Plots

A Recurrence Plot (RP) is a binary plot of a matrix, showing ones when the phase space trajectory of an attractor visits at a different time instance the same area in its phase space within a certain threshold [16]. Mathematically this can be expressed by the Heaviside function in (4) that defines a recurrence matrix:

$$RP_{ij}^{y} = \Theta\left(\epsilon - \|\mathbf{y}_i - \mathbf{y}_j\|\right),\ \mathbf{y}_{i,j} \in R^m,\quad i,j \in 0,N \tag{4}$$

where N is the number of samples, "m" the dimension of the embedded phase space, ||°|| is a norm, ϵ is a threshold, usually around the 10% of the average or of the maximal or mean diameter of the attractor [8]. Three illustrative examples of RPs are reported in Fig.1: a white noise time series (Fig1A), a Lorentz system with null coupling (Fig1B) [17] and a logistic map (Fig1C)[18].

RP can be extended with the notion of the Joint Recurrence plots (JRP), taking directly the Hadamard product (⊙) of two

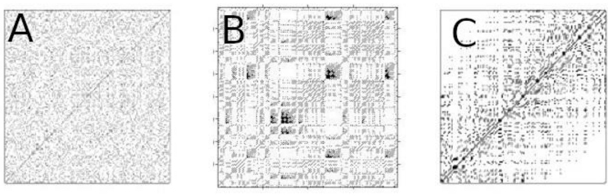

Figure 1 Three illustrative RPs: A) white noise; B) $Lorentz_{28.5} \rightarrow Lorentz_{27.5}$ with null coupling (C=0)[17]; C):logistic map[18].

RPs and so allowing investigating the possible simultaneous occurrences of two quantities, or of two dynamical systems [8].

$$JRP_{xyz} = \overbrace{RP_x \odot RP_y}^{JRP_{xy}} \odot RP_z \tag{5}$$

RPs have indeed the great flexibility of being easily extended to include further "n" quantities by a simple matricial product. Many variants have indeed been introduced for the RR and JRP [8] and recently, the so-called Conditional Recurrence Plots [19] has also been proposed:

$$CJRP_{xy|z} = \mathrm{JRP_{xy}} \odot \left(1 - \mathrm{JRP_{zy}}\right) \tag{6}$$

While (5) allows estimating the same occurrence in the phase space among three quantities, without distinguishing the relative influence between them, (6) has been conceived to filter out the influence of "z" on "y" to better investigate the one between "x" and "y". Technical details can be found in[19], but the main idea behind the CJRP in (6) is that of reducing progressively $\epsilon_{JRP_{yz}}$ while keeping the optimal value for $\epsilon_{JRP_{xy}}$. Indeed, occurrences due to points on the attractor of "z" that are close to those of "y" list a "1" in $\mathrm{JRP_{zy}}$ and then a "0" in $CJRP_{xy|z}$. In this way, only the actual occurrences between "x" and "y" are kept while the ones between "z" and "y" are progressively sifted out and the influence of "z" on "y" minimized.

For each value of $\epsilon_{JRP_{yz}}$, by simply varying the delay between "x" and "y", it is possible to determine the time of maximum interaction between the two quantities considered.

RPs, JRPs and CJRPs may be then used to derive important properties of a dynamical system. In mathematical terms, diagonal lines correspond to trajectories in the phase space visiting the same region at different times. Short diagonals are characteristic of weakly correlated, stochastic or chaotic processes while long diagonals occur for deterministic processes [8]. The so-called recurrence quantification analysis [15] then, provides a number of useful estimators, which are derived from the typological properties of RPs. In the following, the so-called *determinism* (DET) is used as an estimator able to capture information regarding the coupling between dynamical processes. DET is correlated to the periodic behaviour of the systems under study and is defined as the percentage of recurrence points forming the diagonal lines.

Mathematically DET is expressed as [8][15]:

$$DET = \frac{\sum_{l=l_{min}}^{N} lP(l)}{\sum_{l=1}^{N} lP(l)} \tag{7}$$

In (7), N stands for the number of samples, "l" stands for a specific diagonal length, while $P(l)$ represents the number of diagonal lines with the specified length "l". The minimum value for l_{min} is set to $l_{min} = 2$ [8][16]. In this article, the well-established CRP tool [16] has been used to evaluate the RP, their extension, the CJRP and the estimator DET.

3.2 Transfer Entropy and Conditional Transfer Entropy

The Conditional Transfer Entropy (CTE) [7] is a natural extension of the Transfer Entropy (TE) [20] that has been widely applied in the natural sciences to infer the information flow from a candidate driver to a response system in terms of information transfer , i.e as the actual dependence of the "state", defined according to a specific set of features, of a "receiver" on the state of a "source" at a previous time instance[21]. In other words, TE quantifies the amount of information about a variable "y", which can be obtained by knowing another quantity "x". This increase of information can also help in predicting the future of y beyond what is possible to do knowing only its past. The effect of "x" on "y" is equated to the improvement in the prediction of the future of "y" achievable by the information in the past of "x".

In case of time series, the TE is calculated modelling the signals with the formalism of the (discrete) Markov process of order "k" and "l". This means that the probability of measuring a specific value for each quantity considered at the time instance "$n+1$" depends only on a certain number ("k"

or *"l"*) of previously observed states of the quantities themselves [7]. Therefore, the TE quantifies the importance of the knowledge, of a process $\boldsymbol{x}^{(\boldsymbol{k})}$, to predict the occurrence of the state y_{n+1} of a process $\boldsymbol{y}^{(\boldsymbol{l})}$, taking into consideration also the contribution from the memory of y itself. Mathematically the TE represents the conditional mutual information $I(u|v)$ in (8,9) between $\boldsymbol{x}^{(\boldsymbol{k})}$ and $\boldsymbol{y}^{(\boldsymbol{l})}$. The Conditional Transfer Entropy then, simply includes a further quantity $\boldsymbol{z}^{(\boldsymbol{m})}$ as a possible influencer of the outcome of the response quantity $\boldsymbol{y}^{(\boldsymbol{l})}$ [7]:

$$TE_{X\to Y} = I\left(x_n^{(k)}, y_{n+1}|y_n^{(l)}\right) \quad (8)$$

$$CTE_{X\to Y|Z} = I\left(x_n^{(k)}; y_{n+1}|y_n^{(l)}, z_n^{(m)}\right) \quad (9)$$

Eq. (8) can be written for discrete quantities as[20]:

$$TE_{X\to Y} = \sum p\left(y_{n+1}, x_n^{(k)}, y_n^{(l)}\right)\log_2\left(\frac{p\left(y_{n+1}|x_n^{(k)}, y_n^{(l)}\right)}{p\left(y_{n+1}|y_n^{(l)}\right)}\right) \quad (10)$$

In (10) it is clear than that if $x_n^{(k)}$does not improve the understanding of y_{n+1}, i.e $p\left(y_{n+1}|x_n^{(k)}, y_n^{(l)}\right) = p\left(y_{n+1}|y_n^{(l)}\right)$, then TE=0. Using the same formalism of (10), an expression for the CTE has been provided in (11); further details can be found in [22][23] about the formal definition of the CTE.

$$CTE_{X\to Y|Z} = = \sum p\left(y_{n+1}, x_n^{(k)}, y_n^{(l)}, z_n^{(m)}\right) \cdot \log_2\left(\frac{p\left(y_{n+1}|x_n^{(k)}, y_n^{(l)}, z_n^{(m)}\right)}{p\left(y_{n+1}|y_n^{(l)}, z_n^{(m)}\right)}\right) \quad (11)$$

The influence of the selected quantities $x_n^{(k)}$ and $z_n^{(m)}$ on $y_n^{(l)}$ can be studied also at a different time instances spaced of delays d_{xy} or d_{zy} . Both the TE and the CTE are consequently estimators to be maximized.

For continuous quantities the definitions changes slightly and get more complicated. Its discussion is out of the scope of this article and would not improve the understanding of the estimator itself or of the idea behind. However, it is worth considering that the main issue in the estimation of the entropies in eq. (10,11) are the estimates of the probability density functions *pdfs*. Methods have been established to tackle this, like the Kraskov, Stögbauer and Grassberger (KSG) estimator [24] that extends the Kozachenko–Leonenko estimator [25].

To conclude the subsection it has to be mentioned that, in this work, the well-established JIDT tool described in [26] has been used to evaluate both the TE and the CTE.

4. Analysis of H-mode discharges

In this section, the main results obtained with the previously described estimators are reported. It is important to stress that the values of the delays, at which maxima of the considered estimators are observed, are to be considered as the time windows during which the ICRH itself exerts most of its influence on the time evolution of the sawteeth. In other words, the ICRH notching is expected to influence the fast ion population mainly within the time windows ending with this maximum value of the indicators [27][28][29]. This time interval corresponds to the slowing down time of the ions[4][5], i.e the time interval taken by the ions to thermalize on the electrons of the plasma, both for the minority and for the main plasma species.

Consequently, subsection 4.1 provides a short overview of the pulses considered and of the expected estimates obtained using the PION code for the evaluation of the slowing down time of the fast ions, while subsection 4.2 provides the results obtained using the CTE and the CJRP in relation to the PION estimates.

4.1 Experimental discharges considered in the analysis and expected model estimates

In this article, three JET pulses, dedicated to the preparation of the ICRH scenario in support of the DT campaign, have been analysed during the stationary H-mode phases. Table 1 provides the main characteristics of the considered pulses and of the corresponding reference pulses. The main idea behind the use of reference pulses is simple. Since sawteeth are quasi-periodic and can occur naturally also during pacing experiments, we have tried to decouple the natural occurring crashes from the paced ones by using the measurements of the reference pulses. In more detail, for the driver *"x"*, we have considered the total ICRH power injected, while the response quantity *"y"*, describing both paced and natural saweeth, is the central electron temperature measured by the ECE diagnostic.

Table 1 Main parameters for the pulses considered in this analysis. All pulses have been conducted at I=2.2MA and Bt=2.8T. The pulse 94087 differs from 94088,89 by the different percentage of minorities (H%)

Pulse P/R	n_e $[10^{19}m^{-2}]$	$\boldsymbol{P_{NBI}}$ $[\boldsymbol{MW}]$	$\boldsymbol{P_{ICRH}}$ $[\boldsymbol{MW}]$	$\boldsymbol{\nu_{ICRH}}$ $[\boldsymbol{Hz}]$	***H(%)***
94087 *P*	*11.8*	*20.5*	*5.7*	*3*	*2.7*
94091 R	*10.9*	*20.0*	*5.8*		*2.7*
94088 *P*	*11.1*	*20.3*	*6.2*	*3*	*1.3*
94089 *P*	*11.4*	*20.0*	*6.1*	*2.5*	*1.2*
94090 *R*	*11.0*	*20.0*	*5.3*		*1.7*

Finally, the Te measured for the reference pulse, *"z"*, has been used to describe the occurrence of natural sawteeth. Fig.2 shows an example comparing the time traces of the pulse 94089 with the 94090 used as reference.

Experimentally an excellent pacing of the sawteeth for the 94089 pulse was achieved, while the pacing efficiency was not optimal for shot number 94087 and poor for shot number 94088.

One of the possible explanations for such different behaviours is the actual influence of the main plasma second harmonic that absorbs part of the injected power[4]. In other words, not only the minorities, but also the fast ion population of the main ion species might influence the experimental output.

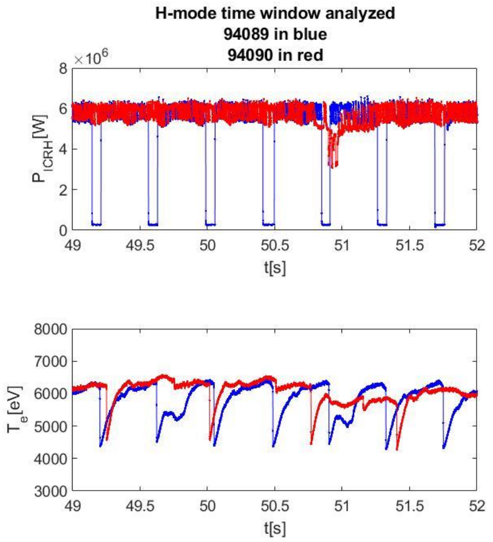

Figure 2 TOP: Total injected ICRH power for the 94089 pulse in blue and for the reference pulse, the 94090 in red; bottom: central electron temperatures, where natural sawteeth can be observed in red for the 94090 time trace and paced ones for the 94089 in blue

Table 2 Main estimates for the slowing down time of ions on electrons for the two main species of the plasma, the minority one (hydrogen) and the deuterium one at the resonance position.

Pulse	$\tau_{eH} \pm \sigma_{\tau_{eH}}$ $[ms]$	$\tau_{eD} \pm \sigma_{\tau_{eD}}$ $[ms]$
94087	(266 ± 40)	(531 ± 80)
94088	(260 ± 25)	(519 ± 50)
94089	(234 ± 26)	(468 ± 52)

To interpret the main results obtained with the estimators used, the PION code has been run to determine the main quantities related to the fast ion populations, especially the slowing down time of the fast ions on the electrons.

For these three pulses the first harmonic of the hydrogen ions ("H1" from now), the second one of deuterium ions ("D2" from now on) and the electrons adds up to 99.9% of the damping power of the ICRH. Furthermore, during the time window considered for the analysis, both resonances overlap at R~3m, i.e $\psi \sim 0; 0.05$ where ψ stands for the normalized flux function. Table 2 provides the PION estimates of the slowing down time of hydrogen and deuterium on the electrons.

4.2 Results obtained using the selected estimators CTE and CJRP

In this subsection, the results obtained by the application of the CTE and of the CJRP are shown. The analysis has been performed over one period of the ICRH frequency, i.e. the delay between the ICRH and the Te time trace has been varied from $[0, 1/\nu_{ICRH}]$, to avoid duplicating the results over a wider time window.

The CTE results are reported in Fig.3 where also the TE is shown for comparison. As it can be seen by simple inspection of the plots in Fig.3, the CTE improves the clarity of the results w.r.t the TE, but no definitive conclusion can be drawn. It is interesting to note that all pulses reveal clearly the importance of the ICRH on the pacing sawteeth for time windows compatible with the slowing down time of the hydrogen (see

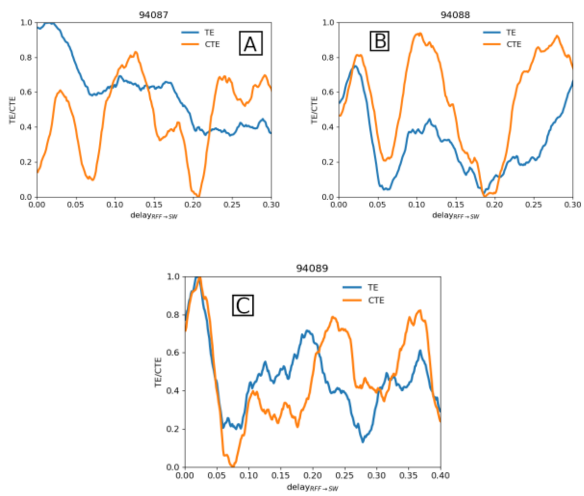

Figure 3 CTE and TE results for the three pulses considered. A) 94087: peaks at 127ms and 240ms emerge more clearly w.r.t the TE analysis where only the ~20ms one can be observed; B) peaks at 110ms and 255ms emerge more clearly w.r.t the TE analysis where again only the ~20ms one can be observed; C)94089: peaks at 236 ms and 380 ms emerge more clearly w.r.t the TE analysis where also in this case, only the ~20ms one can be observed;

Table 2). However, also a strong influence in other time windows, which cannot be directly linked to the fast ions properties, emerges.

A clearer and more comprehensive explanation of the experimental observations can be derived with the CJRP, considering the behaviour of the DET shown in Fig 4.

Pulse 94089 shows clearly two main peaks related to the ICRH. The first one corresponds to the slowing down time of the hydrogen ions, due to the absorption at the H1 harmonic,

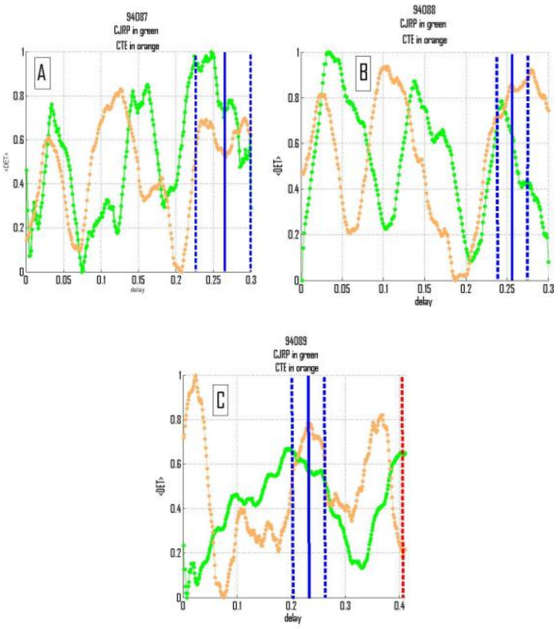

Figure 4 Normalized DET results for the three pulses considered superimposed on normalized CTE results. In blue the estimates and in dashed blue the corresponding upper and lower bounds for H1; in red and dashed red the D2 ones. A) 94087: the relevant peak the H1 has higher relevance w.r.t the previous ones detected; B) 94088: the relevant peak for the H1 has lower relevance w.r.t previous ones detected; C) 94089 shows the importance of the D2 and of the H1;

while another peak can be observed within the lower bound of the estimate of the slowing down time of the deuterons, due to the D2 harmonic absorbion.

On the other hand, both pulses 94088 and 94087 show the importance of the H1 harmonic, but also other local peaks, not easily related to the fast ion populations, can be observed.

Consequently, the results in Fig.4 provide a quite coherent description and allow drawing a series of conclusions, as reported in the following section.

5. Conclusions

In this article, two estimators have been used to support the analysis of dedicated experiments of sawteeth pacing with ICRH modulation: the original CJRP and the more traditional CTE . Both have been implemented to infer the influence of a driving observable (ICRH) on a target (Te with paced and natural sawteeth) minimizing the influence of a third quantity (reference Te with natural sawteeth).

Of the two, the CJRP provides a more coherent description of the analysis performed. Due to the not trivial optimization of the estimator, results of the CTE have been used only to support the CJRP ones.

The results shown in Fig.4 illustrate clearly how pulse 94089 has been properly optimized for the pacing both in term of minority and ICRH modulation. The reported evidence also supports the idea that the ICRH has been able to influence both the minority (H) and the main fast ion distributions (D) of the plasma by the first and the second harmonics respectively.

The results for pulses 94087 and 94088, while not being as clear as the 94089 ones, provide in any case some interesting preliminary information to be considered in comparison with the 94089. Keeping in mind the fact that pulse 94088 differs from the 94089 for the ICRH frequency and that the 94087 and the 94089 for both the frequency and the minority concentration used, then the study performed leads to two alternatives: A) a not optimized ICRH, in terms of either ICRH frequency or minority concentration in the plasma, can lead to effects theoretically still not considered at the moment on the fast ion populations that cause the poor pacing observed for the 94088 and the not optimal pacing of the 94087 (the difference due to the different minority concentration); B) other physical quantities influence the sawteeth occurrences of the paced pulses, i.e. not all spurious influences on the central electron temperature of the paced pulses have been considered.

While the former case goes far beyond the scope of this article, further studies will be dedicated to share some light on the latter conclusion thanks to the CJRP potential to easily include further quantities in the analysis.

In any case, the different behaviours of the CJRP results in Fig4 between pulse 94088 and pulse 94087 can partially explain the poor pacing of discharge 94088 observed experimentally. Considering Fig4B in fact the relative importance of the third peak related to the hydrogen fast ion population is lower w.r.t the two others detected, the opposite occurring for the 94087 discharge.

The results obtained are in any case very promising and therefore, they are expected to provide useful hints for the analysis of the DT2 campaign of JET on specific experiments with ICRH modulations.

Acknowledgements

This work has been carried out within the framework of the EUROfusion Consortium, funded by the European Union via the Euratom Research and Training Programme (Grant Agreement No 101052200 — EUROfusion). Views and opinions expressed are however those of the author(s) only and do not necessarily reflect those of the European Union or the European Commission. Neither the European Union nor the European Commission can be held responsible for them.

References

[1] F. Wagner et al., *Phys Rev Lett*, vol. 49, no. 19, Nov. 1982, doi: 10.1103/PhysRevLett.49.1408.
[2] I.T. Chapman et al 2010 *Nucl. Fusion* 50 102001, doi: doi.org/10.1088/0029-5515/50/10/102001
[3] P. De Vries et al., *Nucl. Fusion* 2011, 51, 053018, doi:10.1088/0029-5515/51/5/053018.
[4] E. Lerche et al 2017 *Nucl. Fusion* 57 036027, doi:10.1088/1741-4326/aa53b6
[5] A. Murari et al 2017 *Nucl. Fusion* 57 126057, doi:10.1088/1741-4326/aa87e7
[6] G. Sugihara et al,. 2012 *Science* **338** 496–500, doi: 10.1126/science.1227079
[7] T. Bossomaier T. et al. , *Springer Nature*, ebook, doi:10.1007/978-3-319-43222-
[8] Marwan N. et al., *Physics Reports*, 2007, 438, 237-439, doi:10.1016/j.physrep.2006.11.001
[9] L G. Eiksson L.-G et al.. (1993) *Nucl. Fusion* **33** 1037, https://doi.org/10.1088/0029-5515/33/7/I07
[10] V. Igochine, Active Control of Magneto-Hydrodynamic Instabilities in Hot Plasmas; Springer: Berlin/Heidelberg, Germany, 2015.
[11] F Porcelli et al 1996 *Plasma Phys. Control. Fusion* 38 2163, doi: 10.1088/0741-3335/38/12/010
[12] I T Chapman et al *2013 Plasma Phys. Control. Fusion* 55 065009, doi:10.1088/0741-3335/55/6/065009
[13] C. Angioni et al 2003 *Nucl. Fusion* 43 455, doi: 10.1088/0029-5515/43/6/308
[14] J P Graves et al 2015 *Plasma Phys. Control. Fusion* 57 014033, doi:10.1088/0741-3335/57/1/014033
[15] J. P. Zblut et al., In Wiley Encyclopedia of Biomedical Engineering, 2006, M. Akay (Ed.). doi:10.1002/9780471740360.ebs1355
[16] N. Marwan et al., Phys. Lett. A, 302(5-6), 2002, 299-307, doi: doi.org/10.1016/S0375-9601(02)01170-2
[17] Krakovská A., (2016), arXiv:1511.00505v2
[18] May R., *Nature* 261, 459, (1976), https://doi.org/10.1038/261459a0
[19] E. Peluso et al., Entropy 2020, 22, 865; doi:10.3390/e22080865
[20] T. Schreiber, PRL, 2000, 85(2), 461-464
[21] M. H. Jakubowski et al. *Phys. Rev. E* 56, 7267, 1997.
[22] J. T. Lizier et al, Chaos 20, 037109 (2010); https://doi.org/10.1063/1.3486801
[23] J. T. Lizier et al, *Phys Rev E*, 2008, doi:10.1103/PhysRevE.77.026110
[24] A. Kraskov et al., *Phys Rev E*, **2004**, *69*, 066138–066153, doi: doi.org/10.1103/PhysRevE.69.066138
[25] L. Kozachenko et al., *Problems of Information Transmission*, **1987,** 23, *9–16*
[26] J. T. Lizier, JIDT:, *Frontiers in Robotics and AI*, **2014,** 1:11, doi:10.3389/frobt.2014.00011
[27] A. Murari et al. *Nucl. Fusion* 56 (2016) 026006 (11pp), doi:10.1088/0029-5515/56/2/026006
[28] A. Murari et al, *Nucl. Fusion* 56 (2016) 076008, doi:10.1088/0029-5515/56/7/076008
[29] A. Murari et al., *Entropy* (2018), 20, 627; doi:10.3390/e20090627